Indian J. Phys. **79(2)**, 183-188 (2005)

AN INTERNATIONAL JOURNAL
IJP

Hydrodynamic modelling of laser ablated plasmas for pulsed laser deposition

Ashutosh Dwivedi
Department of Physics, Maharana Pratap Engineering College, Kanpur-209 217, Uttar Pradesh, India
Email : ashu_dwi@yahoo.com

Received 5 June 2003, accepted 19 October 2004

Abstract : The expansion dynamics of the plasma generated by laser ablation of materials has been described by a hydrodynamic model. The model described here, considers that the interaction of laser beam with the target material can be divided into three separate regimes : (i) laser-target interaction, (ii) laser-plasma interaction and (iii) adiabatic expansion of plasma. The third regime is treated separately for vacuum and ambient gas atmospheres. The results on the hydrodynamical modelling of the laser-generated species in vacuum and in background gas atmosphere, are presented. The thickness distribution of the laser deposited layer in vacuum is found to be related to the initial dimensions of the plasma but independent of both the laser fluence and atomic mass of the target. The angular distribution of the deposits have been deduced as a sum of $\cos^n\theta$. The thickness profiles have been found to show suppression due to ambient gas pressure.

Keywords : Plasma, laser, hydrodynamic modelling.

PACS Nos. : 52.38.Mf, 52.65.Kd, 79.20.Ds

1. Introduction

Pulsed laser ablation and deposition (PLAD) [1] of a material from a target is a phenomenon in which an intense pulsed laser beam is focussed onto the surface of a target material to produce surface heating, vapourization, dissociation, phase changes and excitation. The partially ionized liberated material, or 'ablation plume' is then allowed to settle and form a thin film on a substrate positioned near the target.

In this process, a portion of incident laser energy is transformed into heat energy which ultimately raises the level of electrons on the surface and is transferred to the surrounding surface by electron impact, thus leading to the eruption of high velocity-high pressure plasma plume comprising of electrons, ions and neutral species.

Several successful experimental results obtained in this field, attracted interest in understanding the basic ablation mechanisms. Many theoretical investigations [2,3] had shown the importance of gas phase collisions in interpreting experimental time of flight (TOF) temperature and angular distributions of the ablated particles.

The presence of background gas plays a dominant role during film growth by PLAD [1]. The plasma plume generated during laser ablation flows rapidly with very high velocity, in vacuum. The insertion of an ambient gas greatly influences its propagation and as such, gives retardation to the flowing plasma, thus affecting the plasma plume dynamics. It has been found that the fast components of the plume may cause damage to the growing plasma plume and this can be controlled by the insertion of an ambient gas, upto a certain extent. The pressure and nature or in other words, the mass of the ambient gas modifies drastically the deposited flux [4]. The knowledge of the spatial and angular distribution of this flux can provide a better understanding of the deposition process [5,6]. The quality of the deposited films is critically dependent on the range and profile of the kinetic energy and density of the ablated plumes.

Laser ablated plasmas in a surrounding gas environment are being widely used as a powerful tool for PLD and nano particle production [7–9]. Generally, the diagnostics of pulsed laser ablation and deposition is carried out using optical emission spectroscopy [10,11], absorption spectroscopy, laser induced fluorescence spectroscopy, time of flight mass spectroscopy, interferometers, fast photography and electrostatic probe methods [12,13] like the Langmuir probe diagnostics [14,15] technique.

Several types of lasers such as ArF (193 nm), KrF (248 nm), XeCl (308 nm) and Nd : YAG (355, 532, 1064 nm) have been used to deposit diamond like carbon at the low fluences ranging from 10^8 to 10^{12} w/cm^2 on substrates near ambient temperature [16,17]. Through these experiments, it has been established that diamond like carbon (DLS) films deposited using UV laser, even at low fluences, are of high quality as compared with deposition using longer wavelength. It has also been suggested that diatomic carbon C_2 plays an important role in the fabrication of high quality DLC films [18,19].

Various simulations of laser plasma hydrodynamics in vacuum as well as surrounding gas atmosphere, have been performed in the past. Many fluid dynamic [20,21] models have also been proposed. Kools and co-workers [22,23] have reported the dynamics of laser generated plasma in vacuum and in a background gas at low pressure using Monte Carlo simulation technique. He assumed an elastic collision between background gas atoms and the plume species and considered that the initial expansion was unaffected by the ambient gas. He showed that the increase in pressure thermalises the ablated particles reaching the substrate.

The drag/shock wave model has also been used by various investigators [20,24–26] to explain their experimental results. Wood *et al* [27] had developed an innovative approach for modelling the laser-produced plasmas in low pressure gases, where during the initial expansion, the mean free path may be long enough for the interpenetration of the plume and the background gas. He used a new modelling approach combining multiple scattering and hydrodynamical element and applied it to recently obtained experimental data on silicon ablated into helium and argon gases.

Aden *et al* [28] discussed Knudsen layer model of the laser induced expansion of metal vapour against a background gas pressure. Vertes *et al* [29] introduced a one-dimensional hydrodynamic model based on plasma generation by Inverse Brehmsstrauhlung (IB) in close proximity to the target surface. However, the approach given by Geohegan [30] was a classical one. He took into consideration the shock wave (ideal blast) and the viscosity force (drag force) models.

Nevertheless, as far as we know, only a few researchers [22,25,31,32] are devoted to the modelling of the laser ablation process into a reactive or non-reactive background gas and only the most common configuration is assumed in all of them. In addition, most studies do not accurately describe the thermalization of a laser plume in the background gas and the diffusion of the ablated particles towards the substrate.

For these reasons, simple models which take into account only basic aspects, are often preferred to understand the main features qualitatively. Subsequently, the present work shows the main features of plasma plume propagation qualitatively in vacuum as well as in an ambient gas atmosphere.

In the model proposed here, laser ablation and deposition in vacuum, have been divided into three regimes [33]. The first regime is the evaporation regime in which the interaction of laser radiation with the target material is considered. The second regime comprises of the interaction of the laser fluence with the plasma plume and finally the third regime being the adiabatic expansion of plasma plume. The first two regimes start with the laser pulse and continue until the end of the laser pulse duration, while the last regime starts after pulse termination. The plasma expansion is being simulated using the gas dynamical equation of hydrodynamics and solved for calculating the plasma temperature, spatial distributions and profiles of the ablated material *etc*.

However, for the plasma expansion in an ambient gas, the present work distributes the whole process into four regimes. The first two regimes are similar to the regimes considered in vacuum. The third regime starts after the laser pulse termination. The fourth regime is the interaction of the ambient gas with the expanding plasma plume. In the third regime, the initial plasma expansion is similar to the expansion in vacuum, but as the surrounding gas retards the propagating plume, a fluid membrane formation at the edge of the plume-gas interface occurs and as such leads to a more complex hydrodynamic phenomenon. Using the gas hydrodynamic equations and considering the adiabatic conditions, the plasma expansion in surrounding gas is simulated.

2. Model and simulation

The theoretical aspects of the pulsed laser ablation have been considered to be dependent upon the nature of laser-matter interaction. This interaction plays a crucial role to understand laser ablation as well as pulsed laser deposition of thin films [34]. Among the three regimes considered earlier, the first two regimes are known to be unaffected by background gas and are taken to be isothermal in nature. This helps us in determining the initial conditions for expansion stage. The third regime is anisotropic, three dimensional adiabatic expansion of the laser-generated plasma. It gives rise to the characteristic forward directed nature of the deposition. The evaporation and the isothermal regimes show very different nature of the laser-matter-plasma interaction. In the evaporation regime, the evaporation of target is thermal in nature. In the isothermal regime, the plasma formation, heating and expansion give rise to non-thermal deposition characteristics such as sharply forward directed deposition and kinetic energy of the species becoming much larger than the thermal energy.

The expansion of the plasma can be simulated using gas dynamics equations of hydrodynamics as [35]

$\partial v/\partial t + \nabla\cdot(nv) = 0$, {equation of continuity}

$nM(\partial v/\partial t + (v.\nabla)v = -\nabla P$, {Eulerian equation of motion}

$1/P(\partial P/\partial t + v.\nabla P) - (\gamma/n)(\partial n/\partial t + v\cdot\nabla n) = 0$ {adiabatic equation of state}

$\partial T/\partial t + v.\nabla T = (1-\gamma)T\cdot\nabla\cdot v$ {equation of temperature}

where n is number density, v is velocity, P is plasma pressure and $\gamma(= C_P/C_V)$ is adiabatic exponent. Theoretically [33], the expansion characteristics are dependent on the plasma temperature and in turn, on the energy density of the laser pulse. Pulse energy density affects both transverse as well as perpendicular expansion velocities of plasmas. Due to high density of particles during the earlier stages of plume expansion ($\sim 10^{19} - 10^{20}/\text{cm}^3$), there are numerous collisions and the plasma behaves as a continuum compressible fluid. Here in the present case, we have assumed the linear expansion of plasma. The density and pressure in the plasma decreases linearly from its inner edge. We have also assumed that only atoms desorb from the irradiated surface, in vacuum. The form of laser pulse intensity I was taken as Gaussian. From the equations of hydrodynamics *i.e.* equation of continuity, Eulerian equation of motion, the adiabatic equation of state and equation of temperature, the density (n) of the plasma at any point (xyz) at time t, can be expressed as a Gaussian function given by :

$$n(x,y,z,t) = \left[\frac{n_0}{(2\pi)^{3/2} X(t)Y(t)Z(t)}\right] \exp\left\{-\frac{x^2}{2X(t)^2} - \frac{y^2}{2Y(t)^2} - \frac{z^2}{2Z(t)^2}\right\}, \quad (1)$$

where n_0 is the total number of evapourated particles at the end of the laser pulse ($t = \tau$). $X(t)$, $Y(t)$ and $Z(t)$ are the spatial coordinates of the leading edge of plasma. Fader [36] has deduced that for time scales which exceed four nanoseconds, a Gaussian density profile in the plasma develops. Thermodynamically, the density profile of the plasma should be dependent on the degree of excitation which affects the specific heat capacity ratio γ. The species velocity expression can be given as

$$v(x,y,z,t) = x\left[\frac{\dot{X}(t)}{X(t)}\right]\hat{i} + y\left[\frac{\dot{Y}(t)}{Y(t)}\right]\hat{j} + z\left[\frac{\dot{Z}(t)}{Z(t)}\right]\hat{k}, \quad (2)$$

where $\dot{X}(t) = \frac{dX}{dt}; \dot{Y}(t) = \frac{dY}{dt}; \dot{Z}(t) = \frac{dZ}{dt}$

refer to the expansion velocities of the plasma edges X, Y and Z respectively. The density profile and species velocities have been shown schematically in Figures 1 and 2.

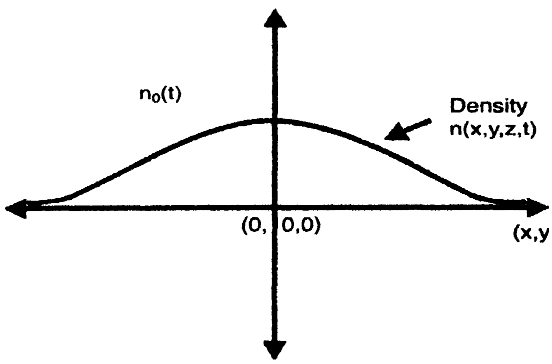

Figure 1. Schematic profile showing the density (n) in the plasma along x direction, which is perpendicular to the target surface.

We have taken into consideration that there are no spatial variations in the plasma temperature, or $\nabla T = 0$. After solving eqs. (1) and (2), the solution which controls the expansion of the plasma comes out to be

$$\ddot{X}(t)X(t) = \ddot{Y}(t)Y(t) = \ddot{Z}(t)Z(t)$$

$$= \frac{kT_0}{m}\left[\frac{x_0 y_0 z_0}{X(t)Y(t)Z(t)}\right]^{\gamma-1} (t > \tau). \quad (3)$$

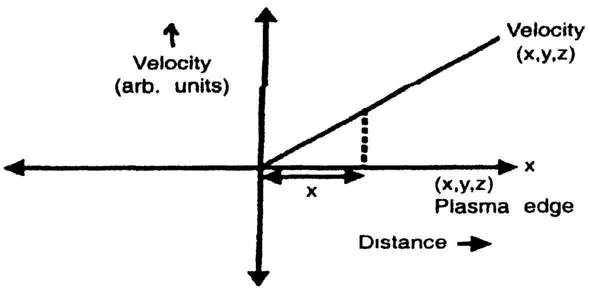

Figure 2. Schematic diagram showing the velocity (v) in the plasma where at the inner edge, v is minimum.

Let m be the mass of the n_0 particle contained in the plasma, which is initially at temperature T_0.

Let M be the amount of matter deposited per unit area at a point m (x,y) of a substrate located at a distance $Z = L$ from the target such that

$$M(x, y, L) = \int_0^{\infty} n(x, y, L, t) v_z(x, y, L, t) dt . \quad (4)$$

Since we have assumed the linear expansion of plasma, so the acceleration terms $\ddot{X}(t), \ddot{Y}(t)$ and $\ddot{Z}(t)$ fall rapidly to zero leading to a constant values of plasma expansion velocity v_x, v_y and v_z. Here, x_0, y_0 and z_0 refer to the initial dimension of the irradiated area. Figures 3 (a and b) show the initial elliptical plasma shape after termination of laser pulse and final shape of the plasma before it strikes the target, respectively.

Now, $X(t)$, $Y(t)$ and $Z(t)$ can be approximated as :

$$X(t) = x_0 + \int X(t) dt$$

$$\approx \int X(t) dt$$

$$\approx V_x t.$$

In vacuum, eq. (4) can be solved directly assuming a linear expansion of plasma such that

$$M(x,y,L) = (n_0 k_x k_y)/4\pi L^2/\{[(x^2 k_x^2/L^2) + (y^2 k_y^2/L^2) + 1]^{3/2}\},$$

where, $k_x = v_z/v_x$ and $k_y = v_z/v_y$.

Let $M_0 = (n_0 k_x k_y)/4\pi L^2$,

such that $M(x,y,L) = M_0/\{[(x^2 k_x^2/L^2) + (y^2 k_y^2/L^2) + 1]^{3/2}\}$. (5)

This equation represents the amount of matter at each point of substrate. It is useful to deduce the nature of the curves corresponding to the same thickness of deposited matter. Thus, the isothickness curves are given as

$M(x,y,L) = K$(constant).

Eq. (5) also can be written as

$$(k_x x/AL)^2 + (k_y y/AL)^2 = 1, \quad (6)$$

where, $A^2 = [M_0/M(x,y,L)]^{2/3} - 1$

which is an ellipse with principal axes,

$a = AL/k_x$ and $b = AL/k$.

Also, $a/b = k_y/k_x = v_x/v_y \approx y_o/x_o$.

This implies that the elliptical material distribution is independent of both mass of ejected species and initial temperature of plasma (T_0) and therefore, of the absorbed laser energy.

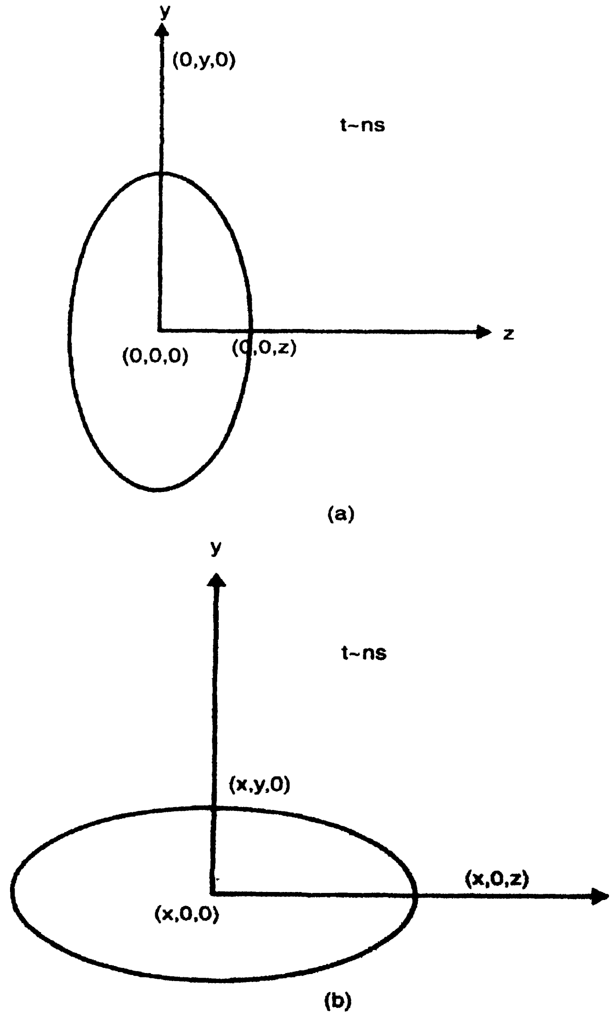

Figure 3. (a) Schematic diagram showing the initial elliptical plasma shape after termination of the laser pulse, (b) Final shape of the plasma before it strikes the substrate.

Eq. (5) along x-axis takes the form

$$M(x,0,L) = M_0/\ [(k_x X/L)^2 + 1]^{3/2}$$

Putting $X = L\tan\theta$

$$M(\theta,L) = [M_0\cos^3\theta/k_x^3](1 - k\cos^2\theta)^{-3/2}$$

$$= \Sigma a_n \cos^{2n+3}\theta$$

where $k = 1 - 1/k_x^2 \approx 1 - (z_0/x_0)^2$.

This implies that K(or a) only depends on initial dimensions of the plasma ($x_0\ y_0\ z_0$). This also explains a different cosine power law following the laser spot size onto the target surface. Experimentalists [6,12] and theoreticians [33], have also found the similar cosine power law at different plasma plume parameters. Figure 4 shows the comparison of our model with the experimental results in vacuum.

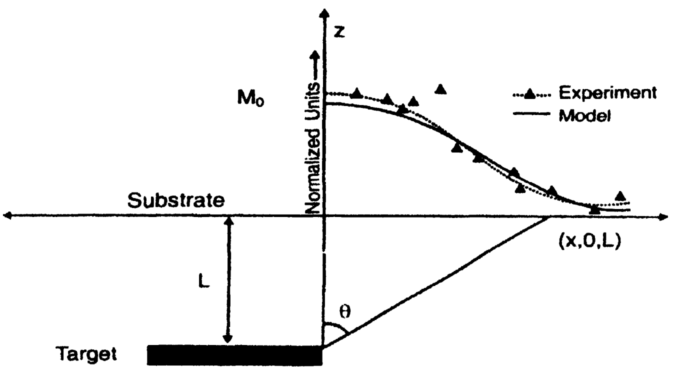

Figure 4. Diagram showing the comparison of the model with experiment in case of vacuum.

In an ambient gas, the density profile is again assumed to be Gaussian such that the gaussian density profile in the gas atmosphere becomes

$$n(x,y,z,t) = [n_0/(2\pi)^{3/2}(X(t) + R(t))(Y(t)$$
$$+ R(t))Z(t)]e^{\{(x2/2(x(t)+R(t))-(y2/2(y(t)+R(t))-(z2/2z(t))\}},$$

where $R(t) = (F_z)/P_z Z(t)$.

We have assumed that the pressure is along z-axis and the dragging force term F_z, considered to be operated in the fourth regime, is given by

$$F_z = m\ddot{Z}(t),$$

where m is the mass of the gas.

It has been found that the term $R(t)$ is only affected while the terms corresponding to coordinates $X(t)$ and $Y(t)$ remain unchanged and the ambient gas effect will start after the plasma plume is formed and it has expanded. Thus, initial plasma plume expansion dynamics has been considered to be linear since it is assumed that the plume expansion hydrodynamics is for vacuum, although the gas application is in process. As the surrounding ambient gas interacts with the propagating plume, a junction in the form of a fluid membrane (called the Knudson layer) is formed. At this point, the propagating plasma plume looses its linearity and gets suppressed affecting the density and velocity profiles (see

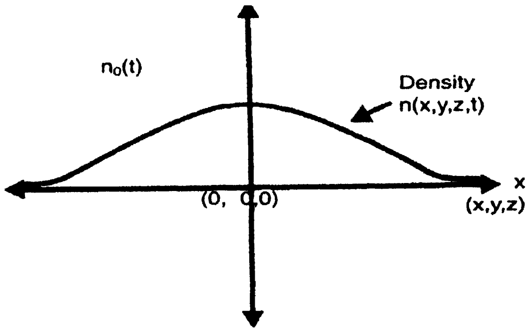

Figure 5. Schematic diagram showing the effect of gas on density of ablated species.

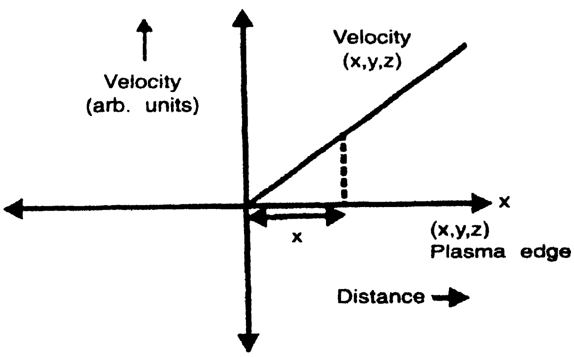

Figure 6. Schematic diagram showing the species velocity profile in gas atmosphere.

Figures 5 and 6). Considering the shifting of points of inflexions of the Gaussian profile, the diagram shows the effect of gas on the expanding plume.

The species velocity profile shows the trend as shown in Figure 6. The ablated material which has high pressure and large velocity tries to push the ambient gas and as such, generates a shock. The shock front propagates through the gas and separates the undisturbed gas from the gas compressed by the expanding vapour. The change in the linear species velocity profile might be due to the fact that the interaction of the plume with the ambient gas reduces the maximum kinetic energy of the ablated atoms and the suppression of the plume may be due to the reduction of the width of the angular distribution. The vapour gas interaction is relatively more marked in the lateral direction than in the radial one which leads to the suppression of the radial expansion.

3. Conclusion

In vacuum, the hydrodynamic equations have been solved to provide information about the density, species velocity and further, plume parameters such as temperature as well as the deposited matter on the substrate. Most interestingly, we found that the elliptical material distribution is independent of both mass of ejected species and the initial temperature of plasma and thus, on the absorbed laser fluence energy. The angular distributions of deposits have been deduced as sum of $\cos^n\theta$ [34,37,38]. In ambient gas environment, the vapour formed by the laser ablation compresses the surrounding buffer gas where shock wave is formed. Due to the surrounding gas, the velocity of the expanding plume is slowed down thus, leading the vapour gas interaction in the radial direction. As we increase the pressure [27], the ablated atom suffers more collisions and hence, more of the atoms get scattered back towards the target. This leads to the reduction of film thickness with increase in pressure.

Acknowledgment

The author would like to thank Dr. R K Dwivedi, Department of Physics, Ch. Ch. College, Kanpur for giving his valuable suggestions from time to time when needed.

References

[1] D B Chrisey and G K Hubler *Pulsed Laser Deposition of Thin Films* (New York : John Wiley) (1994)

[2] R Kelly and R W Dreyfus *Nucl. Instrum. Meth. Phys. Res.* **B32** 341 (1988)

[3] K L Saenger *J. Appl. Phys.* **66** 4435 (1989)

[4] R K Dwivedi and R K Thareja *Surf. Coat. Tech.* **73** 170 (1995)

[5] A Namiki, T Kawai and K Ichige *Surf. Sci.* **166** 129 (1986)

[6] C Champeaux, D Damiani, J Aubreton and A Catherniot *Appl. Surf. Sci.* **69** 169 (1993)

[7] J Muramoto, T Inmaru, Y Makata, T Okada and M Maeda *Appl. Phys. Lett.* **77** 2334 (2000)

[8] R M Mayo, J W Newman, Y Yamagata, A Sharma and J Narayan *J. Appl. Phys.* **88** 6868 (2000)

[9] R M Mayo, J W Mewmann, Y Yamagata, A Sharma and J Narayan *J. Appl. Phys.* **86** 2865 (1999)

[10] R K Dwivedi and R K Thareja *Phys. Rev.* **B51** 7160 (1995)

[11] R K Thareja, Abhilasha and R K Dwivedi *Laser and Particle Beams* **13** 481 (1995)

[12] R K Dwivedi, S P Singh and R K Thareja *J. Mod. Phys.* **B12** 2619 (1998)

[13] D B Geogehan *Pulsed Laser Deposition of Thin Films* (New York John Wiley) **115** (1999)

[14] J Hendron, C M Mahony, T Morrow and W G Graham *J. Appl Phys.* **81** 2131 (1997)

[15] C T Chang, M Hashmi and H C Pant *Plasma Phys.* **19** 1129 (1977)

[16] A A Voevodin, S D Walck, J S Solomon, P J John, D C Ingram, M S Donley and J S Zabinski *J. Vac. Sci. Technol.* **A14** 1927 (1996)

[17] R K Thareja and R K Dwivedi *Phys. Lett.* **A22** 199 (1996)

[18] R K Thareja, R K Dwivedi and Abhilasha *Phys. Rev.* **B55** 2600 (1997)

[19] M L De Giorgi, G Leggieri, A Luches, A Perrone, A Zocco, J Zemek, M Trchova, G Barucca and P Mengucci *Laser Phys.* **8** 270 (1998)

[20] E Gidalevich, S Goldsmith and R L Boxman *J. Phys.* **D33** 2598 (2000)

[21] S I Anisimov, D Baurle and B S Luk Yandruk *Phys. Rev.* **B48** (1993) 12076

[22] J C S Kools *J. Appl. Phys.* **74** 6401 (1993)

[23] J C S Kools, T S Baller, S T DeZwart and J Dieleman *J. Appl. Phys* **71** 4547 (1992)

[24] S H Jeong, R Greif and R E Russo *Appl. Surf. Sci.* **127-129** 1029 (1998)

[25] A V Bulgakov and N M Bulgakova *J. Phys* **D28** 1710 (1995)

[26] J Gonzalo, F Vega and C N Afonso *J. Appl. Phys.* **77** 6588 (1995)

[27] R F Wood, W R Chen, J N Leboeuf, A A Puretzky and D B Geohegan *Phys. Rev. Lett.* **79** (1997)

[28] M Aden, E Beyer and G Herziger *J. Phys.* **D23** 655 (1989)

[29] A Vertes, M De Wolf, P Juhasz and R Gijbels *Anal. Chem.* **61** 1026 (1989)

[30] D B Geohegan *Thin Solid Films* **220** 138 (1992)

[31] T E Itina, W Marine and M Autric *J. Appl. Phys.* **82** 3536 (1997)

[32] Z Kantor and T Szorenyi *E-MRS Spring Meeting (Stratsbourg)* (1997)

[33] R K Singh and J Narayan *Phys. Rev.* **B41** 8843 (1990)

[34] J Neamtu, I N Mihailescu, C Ristoscu and J Hermann *J. Appl. Phys.* **86** 6096 (1999)

[35] Vennard and Street *Elementary Fluid Mechanics* (New York : John Wiley) (2002)

[36] W L Fader *Phys. Fluids* **11** 2200 (1968)

[37] Sushmita R Franklin and R K Thareja *Appl. Surf. Sci.* **15–21** 177 (2001)

[38] A V Gusarov, A G Gnedovets and I Smurov *J. Appl. Phys.* **88** 4352 (2000)